ELECTROMAGNETICALLY GENERATED WAVES ON FREE SURFACE OF LIQUID METAL FOR REFINEMENT PROCESSES

V. Geža, A. Gaile, A. Bojarevičs, M. Mīlgrāvis, Ģ. Zāģeris, and S. Pavlovs

University of Latvia, Raiņa bulvāris 19, LV-1002, Rīga, Latvia

ABSTRACT. One of the most perspective methods to produce solar grade silicon is refinement via metallurgical route. The most critical part of this route is refinement from boron and phosphorus due to high segregation coefficients. One possible approach to remove boron is use of reactive gas on surface of silicon melt. An approach of creating surface waves on silicon melt's surface is proposed in order to enlarge its area and accelerate removal of boron via chemical reactions.
A contactless, electromagnetic approach is proposed for the excitation of the surface waves for electrically conductive materials. This paper describes an experimental study of a table-top model using GaInSn alloy. Surface waves were generated by an alternating magnetic field, produced using a Bitter coil. Additional scaling possibility was investigated by an externally applied static magnetic field. Cases are compared both by analysing acquired photos and by determining the wavelength.
Potential of surface waves to enhance refinement process is investigated numerically showing that certain criteria for surface wave amplitude exist for the refinement to be enhanced.

INTRODUCTION

The exhaustion of fossil fuel resources, global warming, and increased energy consumption all make finding alternative energy sources important. In terms of environmental impact, solar energy is one of the most perspective and attractive sources. However, development of solar power is limited by the solar power costs in comparison to other power sources. As shown in [1], by 2020 the energy cost for solar power is still expected to be higher than for hydro, onshore wind, geothermal, nuclear and even biomass energy sources. Reduction of solar cell production costs is necessary for this technology to develop, and one solution is to reduce the cost of raw materials like polysilicon. Solar cell costs are directly linked to polysilicon production costs, which can be reduced by lowering energy consumption during solar grade silicon (SoG-Si) production.

In many investigations phosphorus removal is found to be the most challenging task, since the purity threshold (< 1 ppm) was not reached [2]. Although, oxidation and slag refinement is simple process for removing phosphorus from silicon, it is insufficient to reach low purity threshold. Mostly used approach for phosphorus removal is evacuation, it is dependent on free surface area and bulk melt stirring. Refinement enhancement can be achieved by superposing DC and AC magnetic fields [3]. Furthermore, this impact creates also mixing effect in the bulk melt, which is also important for boron removal. In comparison, classical induction stirring can enhance only bulk melt mixing, leaving surface area size unchanged.
Known approach for boron removal is blowing of oxidizing gas on free surface [4], and with additional creation of surface waves by means of electromagnetic impact thus creating capillary waves and increasing surface area. Previously mentioned electromagnetic impact technology

(superposition of DC and AC fields) can be used for boron evaporation, because it enhances surface area and stirring.

Highest boron refining rates can be achieved with plasma refining, but it has high energy demand. In reactive gas refining, concentration of boron changes according to first order rate law

$$ln\left[\frac{C_{B,0}}{C_{B,t}}\right] = k_B \frac{A}{V} t$$

Here C_B – boron concentration with indices after comma indicating time, A is the area of interfacial surface between oxidizing gas and silicon melt, V is the volume of silicon melt, t is time, k_B is boron mass transfer coefficient at the surface, measured in μm/s. k_B is determined experimentally and is dependent on oxidizing gas supply rate, type of oxidizing gas and melt temperature. Creation of surface waves would increase A/V ratio, thus speeding up boron removal. Typical k_B values found in literature are 6 – 40 μm/s, and k_P are 2-5 μm/s for phosphorus.

EXPERIMENTAL APPARATUS

The following table-top model was created to investigate electromagnetically excited surface waves in electrically conductive materials. We used GaInSn alloy, also known as Galinstan. It is an eutectic mixture consisting of 68 % gallium (Ga), 22% indium (In) and 10 % tin (Sn). Galinstan was chosen due to its desired physical properties – it is liquid at room temperature, melting point is around +10°C and is of low toxicity and low reactivity.

To demonstrate surface waves with various intensities and the possibility of scaling the technology, both an alternating and a static magnetic field sources are necessary. We used 50 Hz frequency for alternating magnetic field. To demonstrate the effect of scaling, we chose crucibles that have dimensionless frequency close to 1 and greater than 3. Alternating magnetic field source had to be compact as static magnetic field source was built around it. Therefore, alternating magnetic field was created using a Bitter coil principle. This concept provides denser windings with minimum diameter, therefore a stronger magnetic field is achieved if compared to a regular solenoid. The coil consists of 61 circular copper rings of 130 mm inner radius, 154 mm outer, and 2 mm height, see figure 1. The coil is held together using eight threaded rods, cooled by maintaining running water over the outside wall. Over the time of the experimental series electric current strength up to 600 A was used to generate the magnetic field of the strength above 200 mT in the centre of the coil.

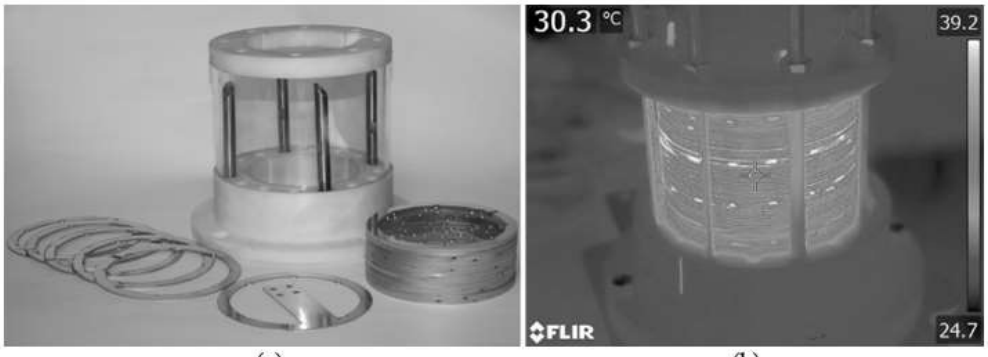

(a) (b)

Figure 1. Bitter coil used for the creation of the alternating magnetic field. (a) the copper plates and the outer shell of the cooling system is demonstrated, (b) a thermal picture of the coil (I = 50 A) without the water cooling

Static magnetic field was achieved using a unique permanent magnet system that consists of 192 pieces of magnets. System is based on Halbach permanent magnet principle. The system has a toroidal shape, the magnets are assembled in layers to create strong magnetic field along its central axis. The magnet system is placed around the Bitter coil, so the magnetic fields are parallel.

During the experiments the surface was filmed and photographed from above at a slight angle, no greater than 10°, image analysing was done using ImageJ [5] to measure the characteristic wave length.

EXPERIMENTAL RESULTS

Cylindrical shaped container was used, $d = 96\,mm$, liquid metal level $h = 61\,mm$ henceforth referred as 10 cm container and $d = 60.7\,mm$, liquid metal level $h = 61\,mm$ henceforth referred as 6 cm container. In the following experiments the container was adjusted in a way that the liquid metal surface was positioned in the middle of the coil where the magnetic field is the strongest.

In this study we compare low magnetic field region, when the alternating magnetic field strength in the centre of the coil is in the range from 20 to 60 mT, the alternating magnetic field has a frequency of 50 Hz. In figure 2. qualitative differences can be seen for the 10 cm container. An increase of the alternating magnetic field strength, with no static field applied, leads to more intense flows in the bulk, thus creating a convex meniscus. The size of the observed surface wave wavelength ranges from 2.3 to 2.7 mm. Meniscus height measurements in the centre of the container give only partial information about the surface deformation, thereof measuring needles were used, showing up to 5 mm height difference for the 55 mT case. Method's precision was not enough to determine the amplitude of the waves.

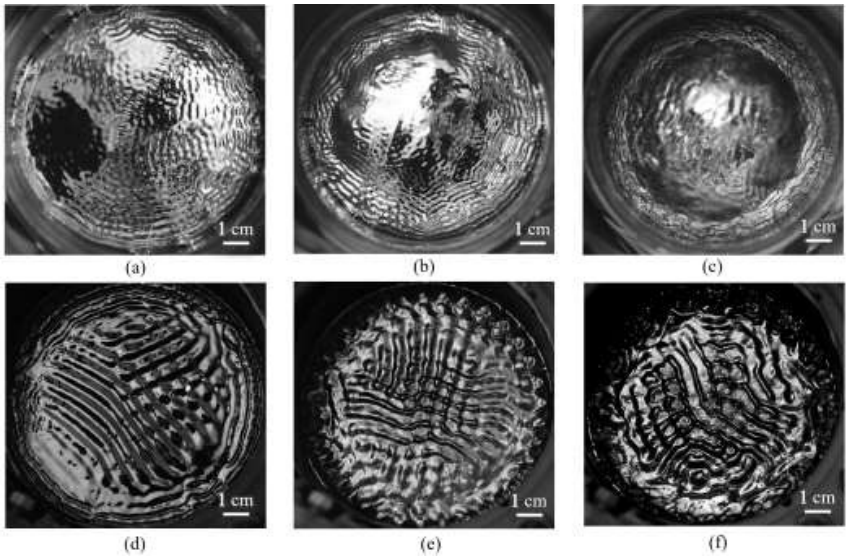

Figure 2. The evolution of waves for a 10 cm container, the magnetic field strength in the centre of the surface is shown for comparison (a) 30 mT, (b) 42 mT, (c) 55 mT, (d) 22 mT with applied external magnetic field, (e) 37 mT with applied external magnetic field, (f) 55 mT with applied external magnetic field

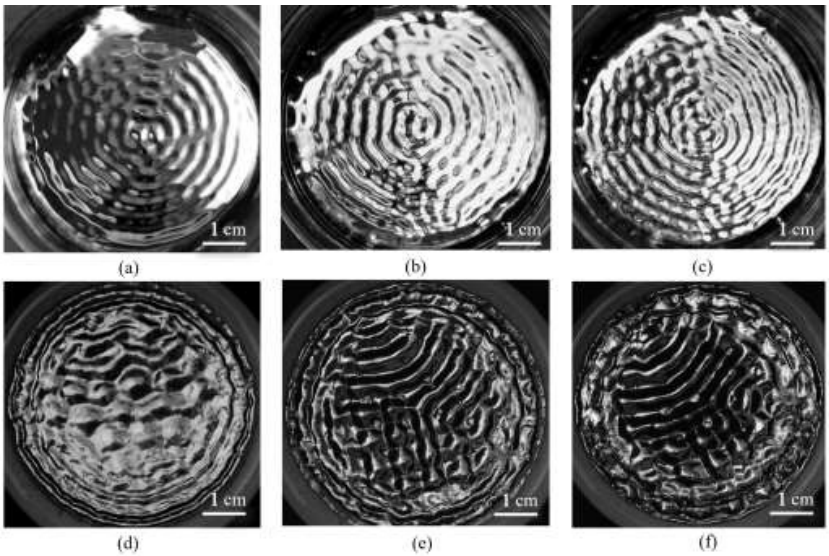

Figure 3. The evolution of waves for a 6 cm container, the magnetic field strength in the centre of the surface is shown for comparison (a) 30 mT, (b) 42 mT, (c) 55 mT, (d) 24 mT with applied external magnetic field, (e) 40 mT with applied external magnetic field, (f) 61 mT with applied external magnetic field

In bottom row of figure 2. static magnetic field has been applied. The flow in the bulk is more suppressed and the meniscus is not forming at the investigated alternating magnetic field values. The waves generated are larger (approximately 6.5 mm) and more intense. The lighting in figure 2 e highlights curling around the edge of the container that was not observed previously without the static magnetic field.

Similar situation can be seen in figure 3. where the evolution of waves for a 6 cm container is shown. Meniscus is not present even at the largest field value presented, indicating that the flow in the bulk is not as intense. The wavelength when no static field is applied is approximately 3.5 mm. If compared to 10 cm container (figure 2 (a)-(c)) the waves are more regular, concentric.

If static magnetic field is applied, the waves break concentric symmetry, and like the 10 cm container, the wavelength increases, it is in range of 5.4 to 6.0 mm. The curling around the edge is not yet fully observable.

As can be seen, the waves in 10 cm container are smaller than in 6 cm container, but in 6 cm container the flow in the bulk is weaker. Both containers showcase greater waves when static magnetic field is applied, leading to acknowledgeable power saving that is desired in production process. For an effective refinement process both wave length and amplitude are of matter. At the moment we have only visually estimated the wave height (amplitude), and can qualitatively say that it increases when the alternating magnetic field is increased.

NUMERICAL SIMULATIONS

For silicon refinement, a system consisting of gas domain with incoming jet (see scheme in figure 4) and molten silicon domain is modelled. The computations of silicon melt flow in crucible and gas flow injected with lance are performed using ANSYS FLUENT package with k–ε turbulence model. Boron concentration both in melt and in gas is traced with UDS (User

Defined Scalar) option in ANSYS FLUENT. Lorentz force, induced by coil is modelled with EMAG module of ANSYS Multiphysics package. Gas supply jet lance diameter is 6.2 mm; gas flow rate is 4 l_N/min, boron-carrying-molecule diffusivity in gas is 3.4 $\cdot 10^{-4}$ m^2/s, boron diffusivity in silicon is 2.4 $\cdot 10^{-8}$ m^2/s.

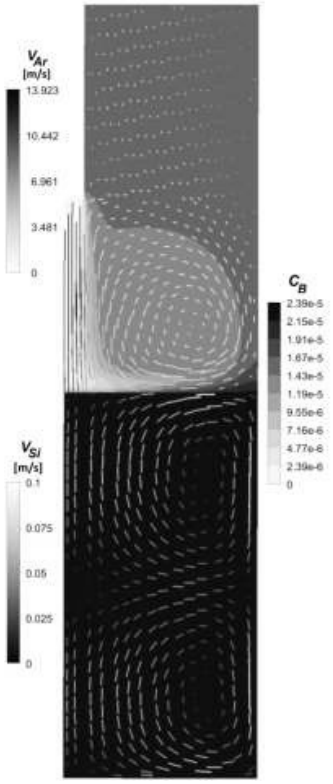

Figure. 4. Modelling of boron removal from silicon with oxidizing gas jet: C_B – boron concentration

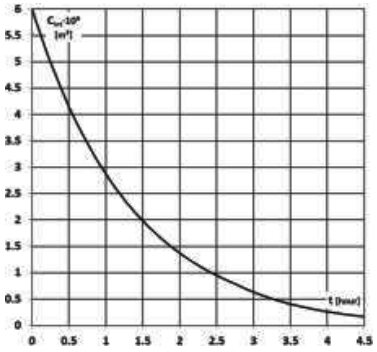

Figure. 5. Boron integral concentration C_{int} in silicon melt as function of silicon refining process time t

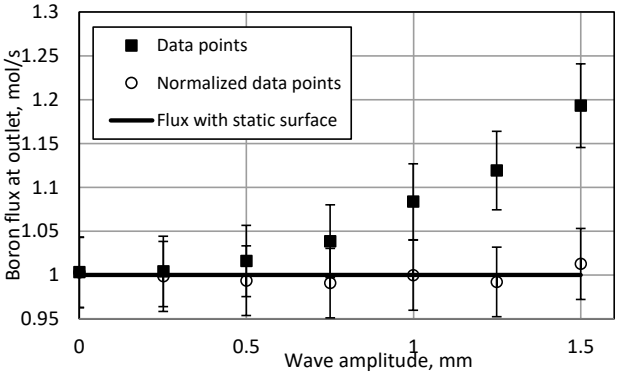

Figure 6. Integral boron flux through outlet dependence on wave amplitude. Error bars – 4% of the value. Data are obtained when steady state is reached

In reality there is a chemical reaction taking action on the surface, where reacting gas oxidizes boron and new molecules are formed which carry boron away from the melt. In this simulation idealized system is used, where one scalar variable was used in both melt and gas domain. In the beginning, fixed concentration of boron in melt is assumed. Then, gas with boron concentration 0 is blown on the surface of silicon, and part of boron is removed.

This simulation was done to estimate the boron mass transfer coefficient k_B at gas–silicon interface. The mean boron concentration in melt during this refinement process simulation is shown in figure 5. The estimated k_B value based on simulation of 5 hours of refinement is 12.7 μm/s. This value is in good agreement with measurement results in [4].

To account the influence of surface waves, a simulation with only gas domain was performed. Gas domain had moving bottom boundary – harmonic wave motion was assigned to it. To

measure the influence of different wave amplitudes and frequencies, a boron flux through outlet was observed.

Surface waves with small amplitudes did not show any enhancement in boron flux in comparison to static gas-silicon interface. The reason for that is strong diffusion, which leads to diffusion length scale comparable to wave amplitude. It turned out that refinement enhancement can be observed only if following criterion is met:

$$A > 4\sqrt{D/f}$$

Here A – wave amplitude, D – diffusion coefficient of boron-carrying molecule in gas, f – frequency of waves. Wave amplitude in this criterion is, however, linked to frequency, therefore it cannot be directly used to estimate required frequency.

Boron flux through outlet of the gas domain was obtained in simulations with different wave amplitudes (figure. 6). There is obvious increase of boron flux with increase of amplitude. However, values normalized on surface area lay on the horizontal line, matching values for flux with static surface. This clearly indicates that boron flux increase is connected with surface area enlargement.

CONCLUSIONS

As the results have shown, aforementioned table-top model demonstrates the possibility of exciting surface waves electromagnetically. Simular wave patterns can be achieved by an alternating magnetic field or by combintion of static and alternating field. Wavelength of the generated waves can be increased to some extent when static magnetic field is applied. External static magnetic field leads to power saving for AC field generation at least 10 times. Results demonstrate the potential to scale technology to the industrial size, but further experiments must be performed.

Increase of magnetic field amplitude leads to increased surface area, which is important for refinement. Simulations show clear dependence of refinement rate on surface area, while certain minimal amplitude is necessary to achieve enhancement of refinement rate.

ACKNOWLEDGEMENT

This work was funded by European Regional Development Fund under contract “Refinement of metallurgical grade silicon using smart refinement technologies” (No. 1.1.1.1/16/A/097).

REFERENCES

[1] U.S. Energy Information Administration (EIA) (2016) – Source // www.eia.gov

[2] Khattak C P, Joyce D B, Schmidt F (2002) *Solar Energy Materials and Solar Cells* 74 77

[3] Bojarevičs A, Beinerts T, Grants I, Kaldre I, Šivars A, Gerbeth G, Gelfgat Yu (2015) *Magnetohydrodynamics* 51 437

[4] Sortland Ø S, Tangstad M (2014) *Metallurgical and Materials Transactions E* 1 211

[5] Rueden C.T. Schindelin J., Hinder M.C., Dezonia B.E. Walter A.E. Arena E.T. Eliceiri K.W. (2017) ImageJ2: ImageJ for the next generation of scientific image data. *BMC Bioinformatics*, 18, 529.